Indian Journal of Engineering & Materials Sciences
Vol. 27, June 2020, pp. 554-563

Effect of red mud proportion on the strength and microstructure of ferrosialate based geopolymer mortar

Bharath Simha Reddy Yeddula & Karthiyaini Somasundaram*

School of Civil Engineering, Vellore Institute of Technology, Chennai Campus, Chennai 600127, India

Received:10 April 2019; Accepted: 30 November 2019

This paper studies the effect of various red mud proportions on the strength and microstructural changes in the ferrosialate geopolymer mortar. The optimum percentage of red mud (RM) has to be found with respect to the molarity of Sodium hydroxide (NaOH) to maintain the suitable alkalinity of the mixture for maximum strength gain. This percentage has been found to be between 20 and 30% RM proportions. From XRD micrographs, it has been found that the crystallinity percentage increased with the increase in red mud content. For oven-cured samples, SEM images showed that, till the red mud replacement reaches 20%, any increase in the red mud leads to denser microstructure and a decrease in intensity of unreactive particles. Beyond that, samples displayed a higher number of undissolved phases. Whereas, for ambientcuring specimens, this limit is found to be 30%. Synergy has to be found among the red mud content, curing type and curing temperature for optimum results. Ferrosialate geopolymer samples has shown 53.34% higher maximum compressive strength than sialate geopolymer samples. The oxide ratios of SiO_2/Al_2O_3 = 4.0 to 4.3, Na_2O/SiO_2 = 0.15 to 0.17 and Fe_2O_3/Al_2O_3 = 0.27 to 0.37 have found to be limits for favouring maximum strength gain.

Keywords: Geopolymer, Mortar, Red mud, Ferrosialate, Fly ash, Sialate

1 Introduction

The alarming levels of global warming and the need for efficient utilization of industrial wastes motivate the present research. Geopolymer is an inorganic material consisting of polymeric chains. Geopolymers consists of aluminosilicate structures of SiO_4 and AlO_4 tetrahedrals[1].The geopolymerization process is divided into three stages, namely, activation or generation of reactive precursors, transportation of reactive precursor ions (generation of monomers), and polycondensation of monomers leading to the formation of semi-crystalline or amorphous geopolymeric gel[2]. Ferrosialate based geopolymer is one of the types of geopolymer in which Fe ions replace some of the Al ions, that is, the geopolymer chain contains [Na, K]-(Si-O-Fe-O-Si-Al)- sequence contrary to typical [Na, K]-(Si-O-Al-O-Si)- sialate/fly ash based geopolymeric sequence. For this type of geopolymer, precursor should be rich in Fe ions, and the maximum replacement of Fe ions in the geopolymeric[3, 4] chain is up to 25%.

Red mud is an industrial waste produced during alumina production. For each ton of alumina production, 1.5 to 1.6 tons of red mud is produced[5]. Globally around 120 billion tons of red mud is produced yearly, and its utilization is very limited due to its high alkalinity[6, 7]. Usually, the pH[8] of red mud ranges between 10 to 13. Because of this, red mud causes severe environmental issues when it is disposed-off as a landfill. It not only damages the surrounding agricultural lands but also pollutes the ground water under it. So, there is an imminent need for the utilization of red mud[9, 10]. This works aims at the utilization of red mud as raw feed for ferrosialate based geopolymer. Red mud serves four purposes in geopolymer concrete. First, it serves as a source of ferrous ions for the formation of a ferrosialate based geopolymer. Secondly, its high pH (pH = 10 to 13) helps in faster leaching of raw feed[8]. Third, the presence of high Na^+ content in it helps for faster leaching. Fourth, Red mud particles fill the micro-gaps in the structure, thereby increasing the density of geopolymer.

Kaze *et al.*[11] studied ferrosialate geopolymers with laterite soil and rice husk ash as raw feed. Similarly, Obonyo *et al.*[12] used tropical red soils for the formation ofa ferrosialate geopolymer. In both cases, ferrosialate geopolymers showed denser microstructure and better strength than conventional (sialate) geopolymers. Very limited literature is available on ferrosialate

*Corresponding author (E-mail: karthiyaini.s@vit.ac.in)

compared to sialate/ fly ash based geopolymers. Also, the influence of red mud proportions on the ferrosialate geopolymers is least focussed.

The oxide ratios of silica and alumina play a crucial role in the strength gain. Even the slight variation in these ratios can have a significant impact on the strength of concrete[13]. Researchers in the past tried to find the ideal range of initial molar ratios of raw feed for fly ash based[1, 14, 15] and metakaolin based geopolymers[13,16,17,18]. As ideal ranges of molar ratiosare dependent on the source material and alkalinity of the solution[19], these cannot be applied for ferrosialate geopolymers. From the literature, it is confirmed that very less work is done to determine the optimal range of molar ratios for ferrosialate geopolymers. This work tries to address these issues by finding the optimal dosage of red mud content along with ideal molar ratios for ferrosialate based geopolymers.

The scope of this work is limited only to study the effect of various red mud proportions on the strength and microstructural changes in the ferrosialate based geopolymer mortar. So the following parameters, NaOH concentration, the solution to binder ratio, sodium silicate to sodium hydroxide ratio (Na_2SiO_3/NaOH), oven curing temperature and resting period are kept constant.

2 Materials and Methods

Red mud is obtained from the aluminium plant, Ms. Hindalco, Belgaum, India. Loss on Ignition (L.O.I) for red mud and fly ash is 10.6% and 0.35%, respectively (Table 1). Excess of moisture content in raw red mud is one of the reasons for showing higher L.O.I. Therefore, red mud in its virgin form cannot be used as a binder. In order to make it into a dry powder, it is oven dried at 80°C. For uniformity, the residue of 150µm sieved dry Red mud sample is used for the study. Fly ash is obtained from Rayalaseema thermal power plant, Andhra Pradesh, India. Sodium silicate (Alkaline grade) with 33% soluble silicates (SiO_2) and Sodium hydroxide pellets of 99% purity are used in work. Throughout the study, Ennore sand/Indian Standard (IS) sand is used as fine aggregate conforming to IS 650[20]. Three grades of sand (grade I: 1 mm to 2 mm, grade II: 0.5 mm to 1 mm, and grade III: 0.09 mm to 0.5 mm) are mixed in equal proportions. Neutral distilled water is used for preparing the alkaline solutions. The physical properties of the raw materials used are shown in Table 2. The specific gravity of the raw feed is found using the pycnometer apparatus. The average particle size of raw materials is found using particle size analyser. The fineness of the raw materials is measured as a specific surface area using Blaine's apparatus. It is observed that average particle size of red mud is much lesser than the fly ash. And also, observed that, red mud is four times finer than fly ash, which helps in faster dissolution process[21]. Also, the pH of red mud (pH=12.1)is found to be 55.3% higher than fly ash (pH=7.79), which helps in boosting the geopolymerization process[8].

Alkali solutions are prepared a day before the casting of specimens. Initially, Sodium hydroxide pellets are mixed and stirred in distilled water. Later once the NaOH solution becomes cool, Sodium silicate is added to it. Mortar specimens for compressive strength tests are prepared and tested conforming to IS 4031 (Part 6)[22]. The chemical composition (from XRF Analysis) of the raw materials is given in Table 1. As the CaO content is very low (1.5%) in the fly ash, it is classified as Class F[23]. Red mud is rich in FeO (41%), which helps in building ferrosialate links. Also, Na_2O content is more red mud (5.47%) than fly ash (0.81%), and this greatly helps in the dissolution of raw feed[8].

Scanning Electron Microscopy (SEM) is used to study the micro structural changes. During X-Ray Diffraction (XRD) analysis, samples are exposed to Cu- K_α radiation, and phase characterization is done using PAN alytical Xpert High score plus[24].

The ranges of the parameters considered for the study are given below. Sodium hydroxide concentration is kept constant at 10 molarity (M). Various trial mixes were conducted and determined the corresponding optimum solution to binder ratio as 0.5. Na_2SiO_3/NaOH ratio is maintained at 2.5. Red mud proportions are varied from 0 to 40 %, with an

Table 2 — Physical properties of the raw materials.

Raw feed	Specific gravity	Average particle diameter (D_{50}) (µm)	Specific surface area (m^2/g)
Red mud	3.1	14.8	12.1
Fly ash	2.24	29.1	3.2
IS sand	2.64	-	-

Table 1 — Chemical composition of raw materials (XRF Analysis).

Material	SiO_2	Al_2O_3	Fe_2O_3	CaO	K_2O	Na_2O	MgO	TiO_2	P_2O_5	SO_3	L.O. I
Red Mud (Virgin state) (%)	10.21	19.4	41.8	2.1	-	5.47	-	8.9	0.32	-	10.6
Fly Ash (%)	64.8	27.66	3.32	1.5	-	0.81	1.1	-	-	0.31	0.35

interval of 5% by weight of the binder. Any red mud proportions above 40% are not giving considerable strength. A resting period of one day is adopted for all the specimens. Both ambient (A), as well as oven curing (H), is considered for the study. 60 °C temperature is maintained throughout the oven curing regime. Ambient cured specimens are air cured till the date of testing. Specimens are tested after 24h, 48h and 72h for oven curing and 14, 28 days for ambient cured samples. A total of 45 mix conditions were considered for the study and their mix quantities (Kg/m^3), as shown in Table 3.

Table 3 — Mix conditions.

S.No.	Mix ID	Fly Ash (kg/m^3)	Red Mud (kg/m^3)	Fine Aggregate(kg/m^3)			Na_2SiO_3 solution (kg/m^3)	NaOH Solution (kg/m^3)	Molarity of NaOH Solution	Type of curing	Curing Regime	Initial Molar Ratio				
				Grade I	Grade II	Grade III						SiO_2/Al_2O_3	Na_2O/SiO_2	H_2O/Na_2O	Na_2O/Al_2O_3	Fe_2O_3/Al_2O_3
1	10R0H24	585	0	585	585	585	208.95	83.58	10	Oven	24 hrs	4.698	0.131	9.795	0.614	0.077
2	10R0H48	585	0	585	585	585	208.95	83.58	10	Oven	48 hrs	4.698	0.131	9.795	0.614	0.077
3	10R0H72	585	0	585	585	585	208.95	83.58	10	Oven	72 hrs	4.698	0.131	9.795	0.614	0.077
4	10R0A14	585	0	585	585	585	208.95	83.58	10	Ambient	14 days	4.698	0.131	9.795	0.614	0.077
5	10R0A28	585	0	585	585	585	208.95	83.58	10	Ambient	28 days	4.698	0.131	9.795	0.614	0.077
6	10R5H24	555.75	29.25	585	585	585	208.95	83.58	10	Oven	24 hrs	4.599	0.136	9.766	0.625	0.123
7	10R5H48	555.75	29.25	585	585	585	208.95	83.58	10	Oven	48 hrs	4.599	0.136	9.766	0.625	0.123
8	10R5H72	555.75	29.25	585	585	585	208.95	83.58	10	Oven	72 hrs	4.599	0.136	9.766	0.625	0.123
9	10R5A14	555.75	29.25	585	585	585	208.95	83.58	10	Ambient	14 days	4.599	0.136	9.766	0.625	0.123
10	10R5A28	555.75	29.25	585	585	585	208.95	83.58	10	Ambient	28 days	4.599	0.136	9.766	0.625	0.123
11	10R10H24	526.5	58.5	585	585	585	208.95	83.58	10	Oven	24 hrs	4.496	0.142	9.737	0.637	0.171
12	10R10H48	526.5	58.5	585	585	585	208.95	83.58	10	Oven	48 hrs	4.496	0.142	9.737	0.637	0.171
13	10R10H72	526.5	58.5	585	585	585	208.95	83.58	10	Oven	72 hrs	4.496	0.142	9.737	0.637	0.171
14	10R10A14	526.5	58.5	585	585	585	208.95	83.58	10	Ambient	14 days	4.496	0.142	9.737	0.637	0.171
15	10R10A28	526.5	58.5	585	585	585	208.95	83.58	10	Ambient	28 days	4.496	0.142	9.737	0.637	0.171
16	10R15H24	497.25	87.75	585	585	585	208.95	83.58	10	Oven	24 hrs	4.393	0.148	9.71	0.649	0.22
17	10R15H48	497.25	87.75	585	585	585	208.95	83.58	10	Oven	48 hrs	4.393	0.148	9.71	0.649	0.22
18	10R15H72	497.25	87.75	585	585	585	208.95	83.58	10	Oven	72 hrs	4.393	0.148	9.71	0.649	0.22
19	10R15A14	497.25	87.75	585	585	585	208.95	83.58	10	Ambient	14 days	4.393	0.148	9.71	0.649	0.22
20	10R15A28	497.25	87.75	585	585	585	208.95	83.58	10	Ambient	28 days	4.393	0.148	9.71	0.649	0.22
21	10R20H24	468	117	585	585	585	208.95	83.58	10	Oven	24 hrs	4.284	0.154	9.682	0.661	0.27
22	10R20H48	468	117	585	585	585	208.95	83.58	10	Oven	48 hrs	4.284	0.154	9.682	0.661	0.27
23	10R20H72	468	117	585	585	585	208.95	83.58	10	Oven	72 hrs	4.284	0.154	9.682	0.661	0.27
24	10R20A14	468	117	585	585	585	208.95	83.58	10	Ambient	14 days	4.284	0.154	9.682	0.661	0.27
25	10R20A28	468	117	585	585	585	208.95	83.58	10	Ambient	28 days	4.284	0.154	9.682	0.661	0.27
26	10R25H24	438.75	146.25	585	585	585	208.95	83.58	10	Oven	24 hrs	4.172	0.161	9.655	0.674	0.323
27	10R25H48	438.75	146.25	585	585	585	208.95	83.58	10	Oven	48 hrs	4.172	0.161	9.655	0.674	0.323
28	10R25H72	438.75	146.25	585	585	585	208.95	83.58	10	Oven	72 hrs	4.172	0.161	9.655	0.674	0.323
29	10R25A14	438.75	146.25	585	585	585	208.95	83.58	10	Ambient	14 days	4.172	0.161	9.655	0.674	0.323
30	10R25A28	438.75	146.25	585	585	585	208.95	83.58	10	Ambient	28 days	4.172	0.161	9.655	0.674	0.323
31	10R30H24	409.5	175.5	585	585	585	208.95	83.58	10	Oven	24 hrs	4.057	0.169	9.627	0.687	0.377
32	10R30H48	409.5	175.5	585	585	585	208.95	83.58	10	Oven	48 hrs	4.057	0.169	9.627	0.687	0.377
33	10R30H72	409.5	175.5	585	585	585	208.95	83.58	10	Oven	72 hrs	4.057	0.169	9.627	0.687	0.377
34	10R30A14	409.5	175.5	585	585	585	208.95	83.58	10	Ambient	14 days	4.057	0.169	9.627	0.687	0.377
35	10R30A28	409.5	175.5	585	585	585	208.95	83.58	10	Ambient	28 days	4.057	0.169	9.627	0.687	0.377
36	10R35H24	380.25	204.75	585	585	585	208.95	83.58	10	Oven	24 hrs	3.938	0.178	9.6	0.7	0.433
37	10R35H48	380.25	204.75	585	585	585	208.95	83.58	10	Oven	48 hrs	3.938	0.178	9.6	0.7	0.433
38	10R35H72	380.25	204.75	585	585	585	208.95	83.58	10	Oven	72 hrs	3.938	0.178	9.6	0.7	0.433
39	10R35A14	380.25	204.75	585	585	585	208.95	83.58	10	Ambient	14 days	3.938	0.178	9.6	0.7	0.433
40	10R35A28	380.25	204.75	585	585	585	208.95	83.58	10	Ambient	28 days	3.938	0.178	9.6	0.7	0.433
41	10R40H24	351	234	585	585	585	208.95	83.58	10	Oven	24 hrs	3.814	0.187	9.572	0.714	0.491
42	10R40H48	351	234	585	585	585	208.95	83.58	10	Oven	48 hrs	3.814	0.187	9.572	0.714	0.491
43	10R40H72	351	234	585	585	585	208.95	83.58	10	Oven	72 hrs	3.814	0.187	9.572	0.714	0.491
44	10R40A14	351	234	585	585	585	208.95	83.58	10	Ambient	14 days	3.814	0.187	9.572	0.714	0.491
45	10R40A28	351	234	585	585	585	208.95	83.58	10	Ambient	28 days	3.814	0.187	9.572	0.714	0.491

3 Results and Discussion

The effect of red mud (RM) proportion on the strength and the microstructure of geopolymer matrix in different curing conditions are discussed in the following sections. Also, the difference in the behaviour of sialate/fly ash and ferrosialate/ red mud based geopolymers are correspondingly compared.

3.1 Influence of Red Mud Proportion

Compressive strength test results with varied red mud replacements for oven curing and ambient curingregimes, are shown in Fig. 1 and Fig. 2, respectively. For the oven curing regime, maximum compressive strength among the samples with 0, 10, 20, 30 and 40% RM is 15.39, 21.1, 23.86, 21.77, and 16.04 MPa, respectively. Similarly, for an ambient curing regime, these values are 10.57, 13.14, 15.56, 20.02 and 13.49 MPa, respectively. It is observed that, as the red mud is added to the mixture, the strength of the samples started increasing, reaches an optimum value and then strength started declining.

And also, it is found that this optimum value of red mud replacement is dependent on the curing conditions. For oven curing and ambient curing, these optimum values observed are 20% (Fig. 1) and 30% (Fig. 2), respectively.

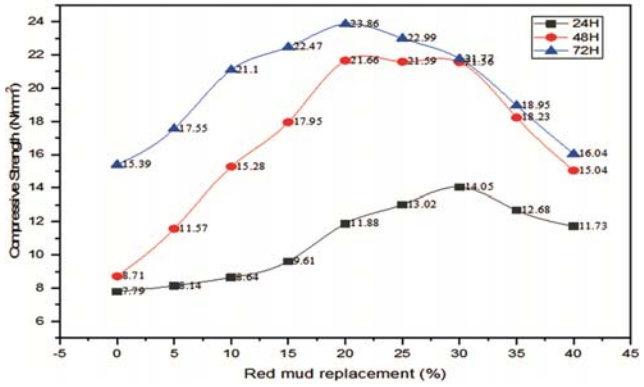

Fig. 1 — Compressive strength-oven cured samples.

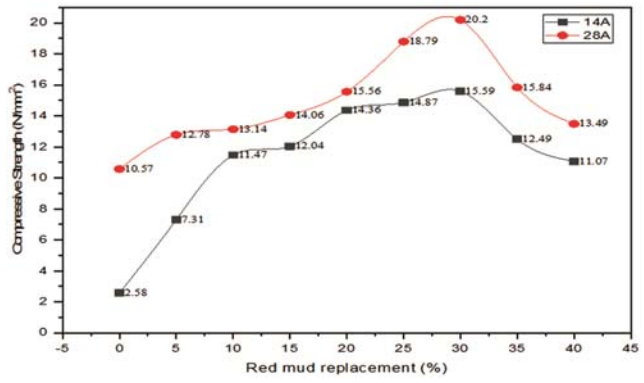

Fig. 2 — Compressive strength-ambient cured samples.

At the lower dosages of RM, the alkalinity of the mixture is not sufficient enough to fully dissolve the raw feed. This leads to the formation of partially dissolved raw feed, as confirmed by the SEM images (Figs.3d and 4b). Till the optimum RM replacement, the alkalinity of RM boosted the dissolution process and helped in the formation of ferrosialate links[10]. And this leads to the formation of a denser microstructure (Figs. 3f and 4c). This might be one of the reasons for an incremental trend in the strength till optimum dosage of RM. Maximum compressive strength attained by sialate (0% fly ash) and ferrosialate (5 to 40% RM) samples are 15.39 and 23.86 MPa, respectively. This shows that, ferrosialate geopolymers showed 53.34% higher maximum compressive strength than sialate geopolymers.

As the red mud is one of the contributors to alkalinity, the alkalinity of mixture increases with red mud content[25]. Higher alkalinity leads to the faster dissolution of raw feed[5], and this process helps in formation of higher geopolymer content. This is one of the reasons for ferrosialate geopolymers showing higher compressive strength than fly ash based geopolymers, at the similar NaOH molarity (10M). This is supported by the SEM images (Figs. 3b, 3f, 4a, and 4d) and XRD graphs (Figs. 5a, 5c, 6a, and 6c)

As the red mud content in the mixture crosses the optimum value, the alkalinity of the mixture is so high that it hinders the geo polymerization process (during the condensation phase) by forming $[SiO_2(OH)_2]^{2-}$[2, 26]. $[SiO_2(OH)_2]^{2-}$ is responsible for the formation of shorter oligomers, which finally leads to lesser strength. This is one of the reasons for strength loss beyond the optimum value of red mud replacement. Red mud addition also increases the crystalline content, which is confirmed by XRD graphs (Fig. 5d and 5f), this might also be one of the reasons for strength loss beyond 30% RM replacement.

Ferrous ions from the red mud can replace only 25% of the total aluminium ions in the polymer chain[26]. So, the addition of red mud beyond a certain point does not helps in the formation of ferrosialate links. Red mud comprises of finer undissolved particles compared to fly ash[9]. So, beyond the optimum dosage of red mud, it only acts as unreacted filler [4], and this is confirmed by the SEM images (Figs. 3g and 3h). The presence of an excess of finer fillers in the mixture leads to the blockage of pores that are used for evaporation. This condition is not

preferable when the rate of evaporation is high[27] (oven curing regime), as it may lead to internal pressure in the gel and cause crack formation[28]and ultimately leading to lesser strength of the specimens. This constraint does not apply to the ambient curing regime, where the rate of evaporation is slow. This might be the reason for oven cured samples(20% RM) showing lesser optimum red mud proportions than the ambient cured (30% RM) samples.

For oven curing conditions, the maximum compressive strength observed for 24, 48, and 72 hours of curing (Fig. 1 and Fig. 2) are 14.05, 21.66, and 23.88 MPa. Hence, it observed that, as the oven curing duration increases, there is an increase in strength. A similar trend is observed by BV Rangan[29] for sialate specimens. The maximum strength gained by the sialate and ferrosialate specimens between 24 hrs and 72 hrs of curing regime is 97.5% and

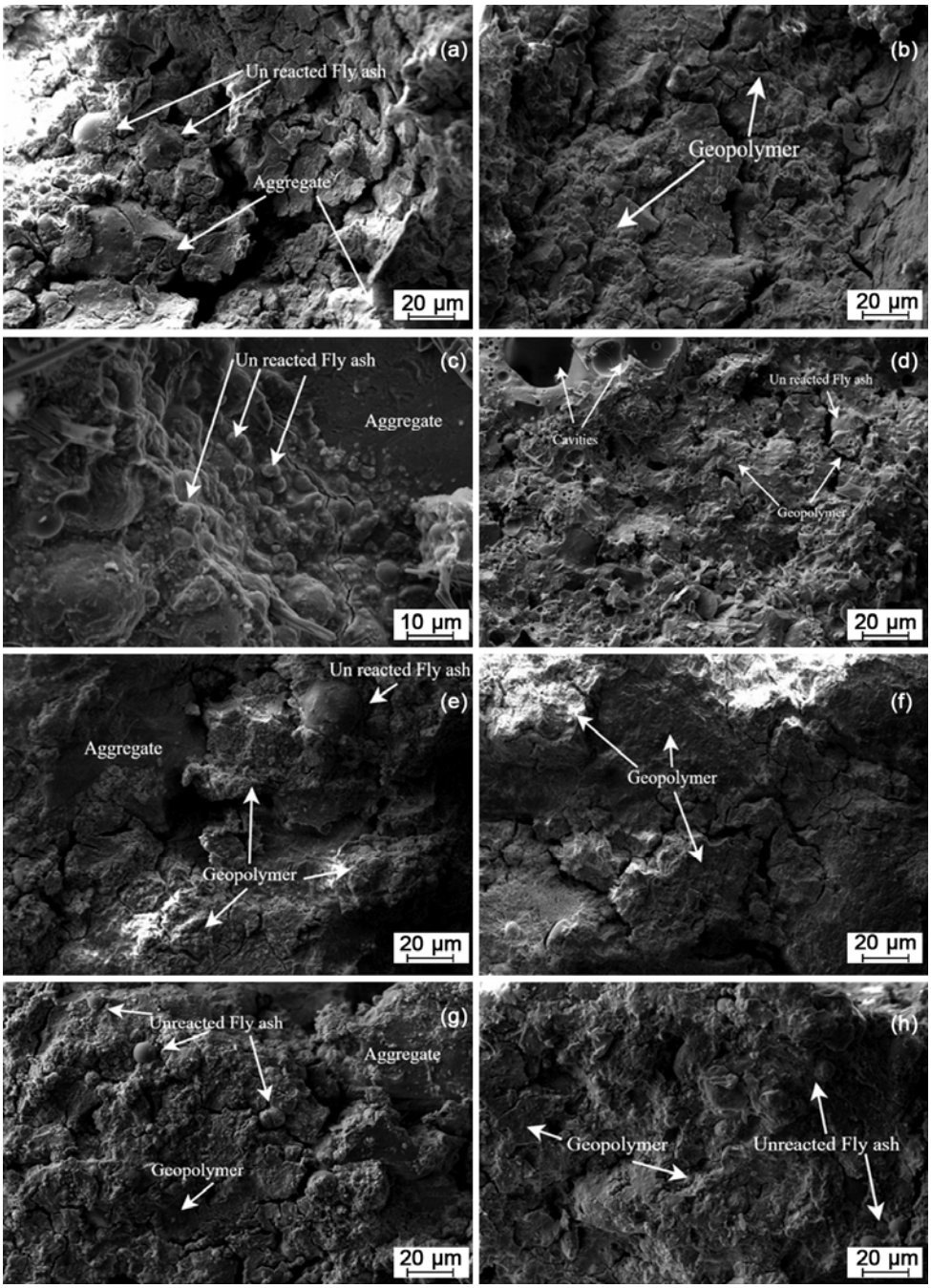

Fig. 3 — SEM micrograph- oven cured samples.

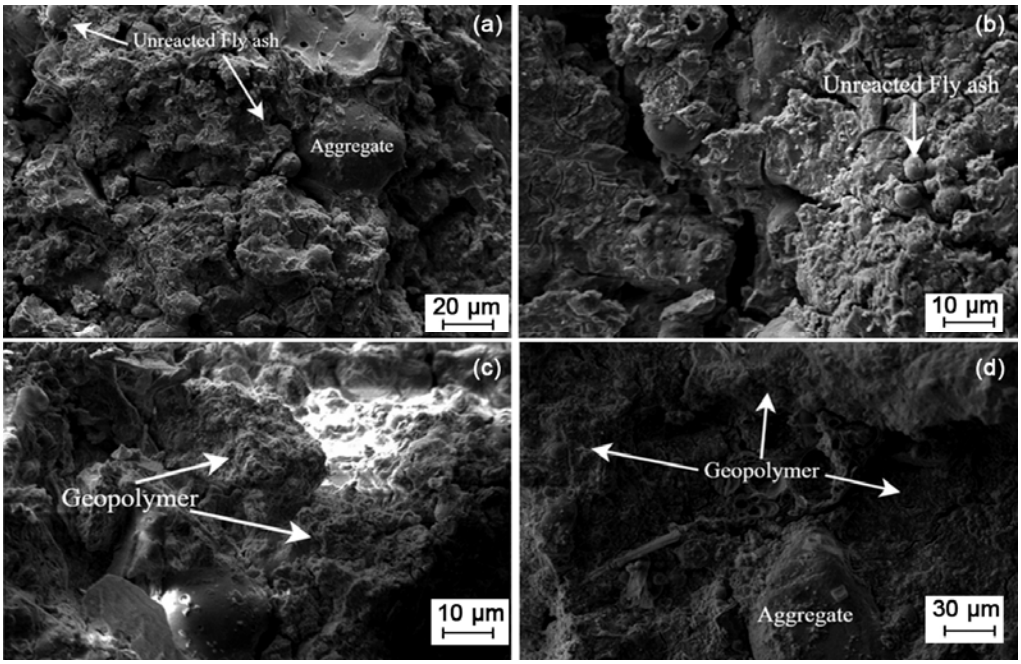

Fig. 4 — SEM micrograph- ambient cured samples.

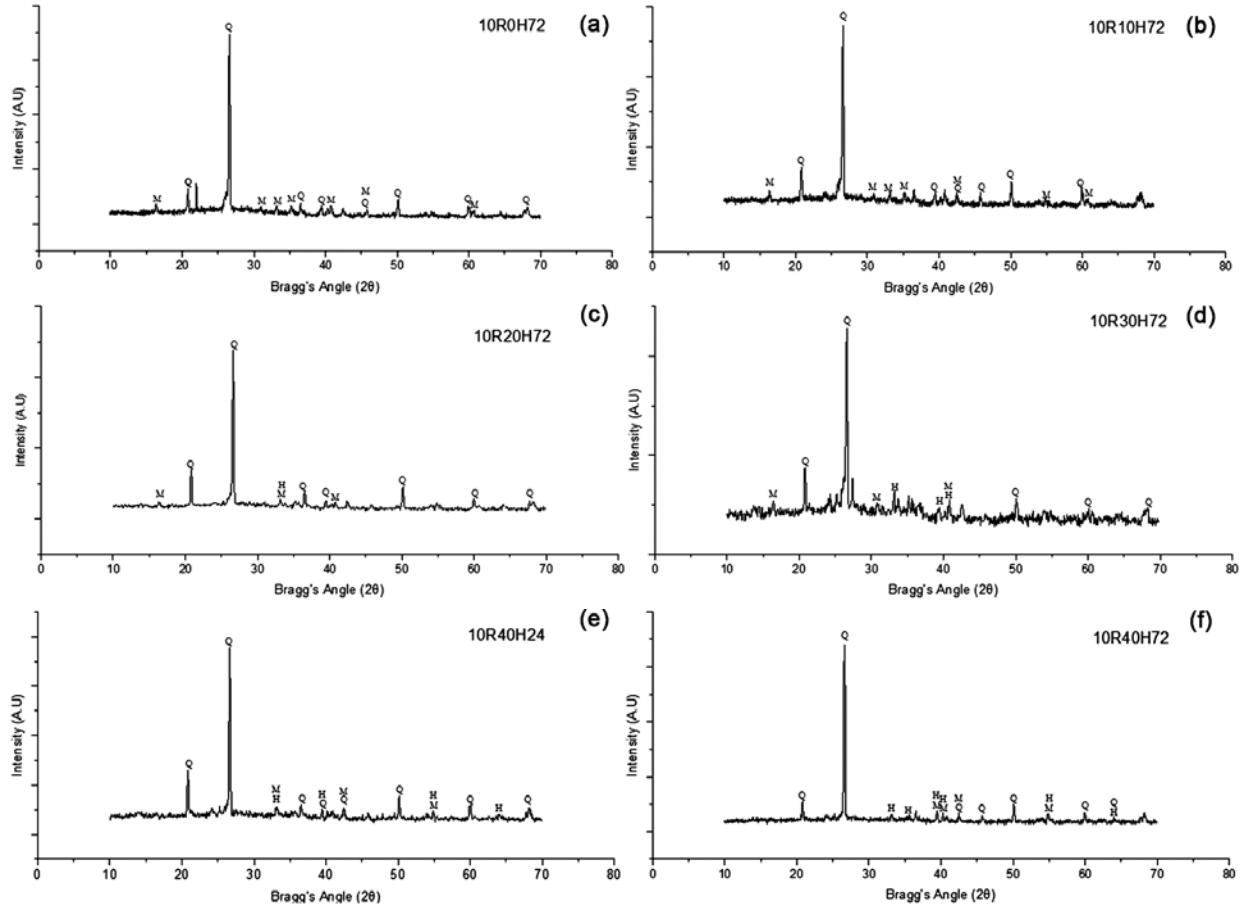

Fig. 5 — XRD of 72 h oven cured samples.

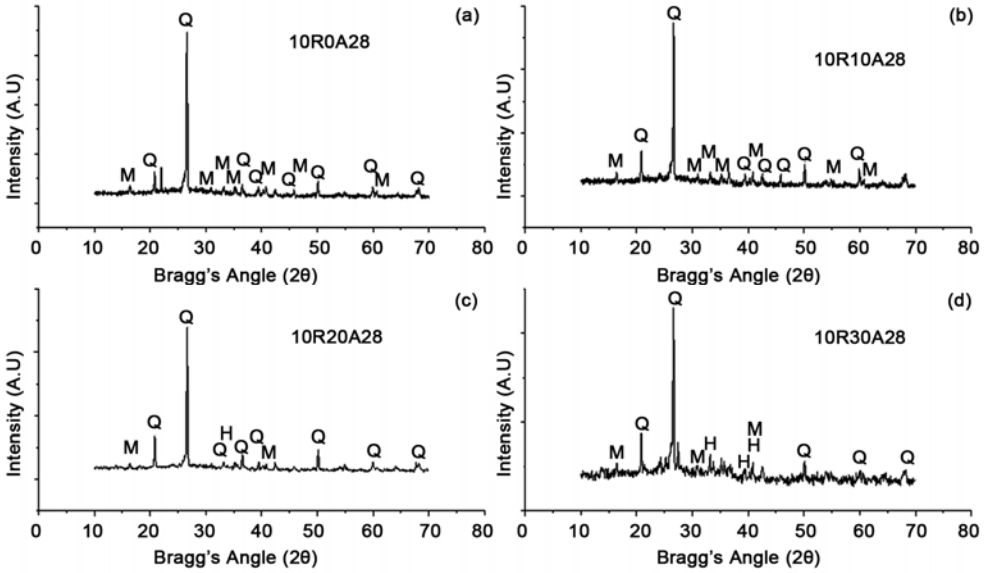

Fig. 6 — XRD of ambient cured specimens.

69.9%, respectively. It shows that, for ferrosialate geopolymers, the rate of strength gain decreases as the duration of curing increases. This is because most of its strength is gained at the early stages of curing.

Similarly, among the ambient cured samples (in between 14 days and 28 days of curing regime), these values are 350% and 29.5%. This shows that ferrosialate geopolymers attain most of its strength at 14 days. Whereas, sialate geopolymers failed to attain the serviceable strength. Therefore, it is confirmed that, for any type of curing, ferrosialate geopolymers requires lesser curing time than the conventional fly ash/sialate geopolymers for strength gain.

3.2 Initial Molar Ratios

Initial molar ratios with their corresponding mix proportions are shown in Table 3. The initial oxide ratio places a crucial role in strength development[29]. Higher silica to alumina ratio leads to the formation of larger Si-O-Si bonds[1], which favours higher strength. But, as the rate of silicate ratio increases, it retards the condensation process, ultimately hindering the geopolymerization[30]. That is, beyond a certain point, a high SiO_2/Al_2O_3 ratio in the mixtures leads to lesser strength[31]. This might be one of the reasons for mixtures with $SiO_2/Al_2O_3 > 4.3$ (RM < 30%) showing lesser strength.

Al ions in the alkaline medium dissolve at a faster rate compared to Si ions, implying that the presence of a high amount of Al ions leads to higher strength[32, 33]. But, excess of Al_2O_3 content is also not preferable as Al_2O_3 increases the crystalline content in the mixture, which finally leads to a reduction in strength[33]. An increase in the crystalline content with the increase in the Al_2O_3 content is confirmed by the XRD graphs (Figs. 5c and 5f). This might be one of the reasons for mixtures with $SiO_2/Al_2O_3 < 3.9$ (RM > 30%) showing lesser strength.

Compared to Si and Al ions, Fe ions are harder to dissolve in the alkaline medium[34]. Also, in a ferrosialate geopolymer, Al atoms in the polymer chain can be replaced by Fe atoms only by 25%[4]. Therefore, the presence of Fe_2O_3 beyond a certain range is not suitable for geopolymerization. From the strength results, it is found that $Fe_2O_3/Al_2O_3 > 0.37$ is reducing the strength.

So, considering all these factors, finding the optimum percentage for oxide ratios of silica, alumina, and ferrous are necessary for the maximum dissolution of raw feed and optimum geopolymerization. By analysing the results of strength tests along with other characterization test results, these optimum ranges are found to be SiO_2/Al_2O_3 = 4.0 to 4.3, Na_2O/SiO_2 = 0.15 to 0.17, Fe_2O_3/Al_2O_3 = 0.27 to 0.37.

3.3 XRD Analysis

XRD analysis is done to find the changes in the crystalline phases and also to find the relative amount of amorphous content in the geopolymer matrix. XRD graphs of the raw materials are shown in Fig. 7. The dominant crystalline peaks identified in the fly ash sample are Quartz (Q) and Mullite (M). Whereas for

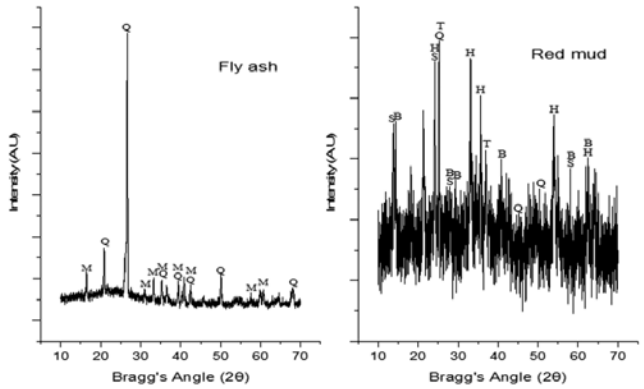

Fig. 7 — XRD of raw materials.

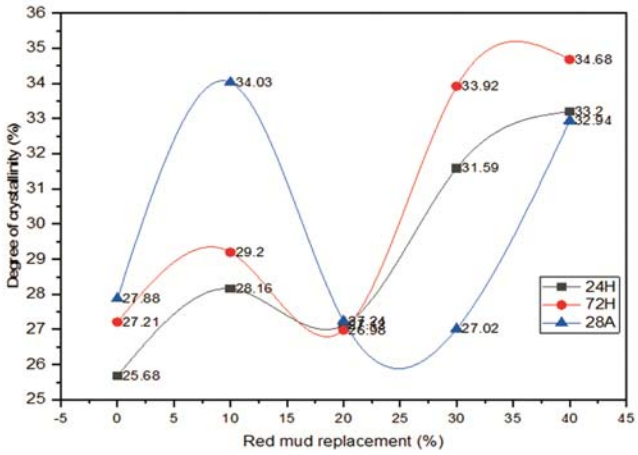

Fig. 8— Degree of crystallinity.

the red mud sample, peaks identified are Quartz, Mullite, Hematite (H), Boehmite (B), Sodalite (S), and Titanium dioxide (T). The hump between 15 to $36^0$2Theta which is a characteristic signature for amorphous content[35], is present in fly ash, whereas it is least visible in red mud. Even after the geopolymerization, samples with maximum strength comprises of hematite peaks (Fig. 5f), which its origin is from red mud. This confirms that red mud is more of a crystalline nature than fly ash[35-37].

The amount of crystalline content in the geopolymer is quantitatively measured using the degree of crystallinity (DOC) technique. The degree of crystallinity can be found using the Eq. (1)[38, 39]. The amount of crystalline content is indirectly proportional to the amorphous phase in the matrix. The amorphous phase implies the geopolymer content present in the matrix[40]. That is, lower is the DOC value, the higher are the chances of formation of geopolymer paste. The changes in the percentage of crystallinity due to the change in curing type and curing duration are shown inFig. 8.

$$\text{Degree of Crystallinity} = \frac{\text{Crystalline Area}}{\text{Area under all the phases}} \quad \ldots(1)$$

The XRD micrographs of 24 hrs, 72 hrs oven cured samples, and ambient cured samples are shown in Figs. 9, 5 and 6 respectively. As the red mud proportion increases in the mix, a greater number of crystalline peaks are visible. This is because red mud inherits higher insoluble phases than fly ash[41]. But at 20% and 30% replacement of red mud for oven and ambient cured regime, respectively, there is a decrease in the degree of crystallinity. Also, for these proportions, the amorphous hump is visible, and peak widths are broadened in the XRD graphs (Figs. 5d and 6d). This indicates the formation of a geopolymer binder[40]. It is also clearly reflected in strength results by showing the highest compressive strength for these mix proportions.

This is because in this situation, parameters like curing type, curing temperature and curing age are at optimum, which favours geopolymerization. Therefore, the synergy among these parameters is crucial for attaining optimum strength.

Beyond 30% replacement of red mud, amorphous hump disappears, and crystalline peaks are predominant with much stiffer peaks (Fig. 5f). This could mean that some of the phases in the red mud are not involved in geopolymerization and serves only as fillers for strength gain, and also dissolution is insufficient thereby hindering geopolymerization[27]. This is confirmed from the SEM images (Figs. 3g and 3h). It is also seen that; DOC followed an incremental trend for the samples with RM content greater than 30%. This means that geopolymer binder content started decreasing when the RM replacement crossed 30%. This might be the reason for the decrement in strength beyond 30% replacement of red mud.

It is observed that the intensity of crystalline peaks is more for ambient samples (Fig. 6d) than 72 hrs oven cured samples (Fig. 5d). Also, the DOC value of ambient cured samples is higher than the 72 hrs cured samples. This implies that ambient samples contain more undissolved content than oven cured samples, which is clearly observed in SEM images (Figs. 3f and 4c). This is the reason for oven cured samples showing higher compressive strength than the ambient samples.

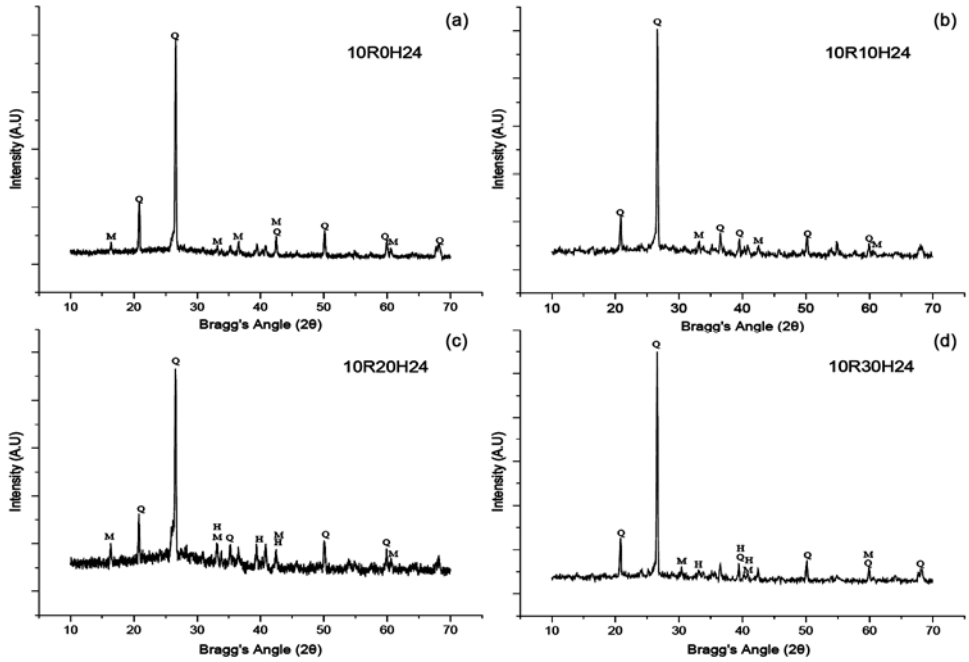

Fig. 9 — XRD of 24 h oven cured specimens.

3.4 SEM Analysis

SEM micrographs for oven cured and ambient cured samples are shown in Figs. 3 and 4 respectively. The sample that is used for SEM imaging is a disturbed sample collected from the specimen after subjecting it to a compression test. This may be the reason for some of the samples showing microcracks.

For the samples with 100% fly ash (Fig. 3a), spherical shapes are predominant, which indicates unreacted raw feed. This shows that the alkalinity of the mixture is insufficient to dissolve the raw feed completely. Unreactive particles are present mostly in all the samples, but its intensity decreases with an increase in red mud replacement. As the red mud dosage is increased, samples showed a denser microstructure. For oven cured samples, this pattern is followed until the red mud replacement reaches 20%. Once the dosage of RM crossed 20%, non-reactive phases (Fig. 3g) are dominant in the microstructure. And these phases are crystalline in nature, which is confirmed by the XRD plots (Fig. 5d). This validates the reason for the decrease in the strength from 20% to 40% RM. A similar scenario is observed for the ambient cured samples but can be seen only after 30% RM replacement. Even the sample with the highest strength displayed few unreacted phases (Fig. 3d), and this is because of non-reactive/ undissolved phases in raw materials (fly ash and red mud)[42].

In both the curing regimes, as the duration of curing is increased, more dissolution of raw feed is seen. This results in a denser microstructure and thereby leading to higher compressive strength. But in ambient cured samples, a larger number of undissolved phases are observed than the oven cured samples. This explains the reason for 28 days of ambient cured samples showing lesser strength compared to 3-day oven-cured samples.

Ferrosialate samples (Figs. 3f and 4d) showed a denser microstructure with least undissolved phases than sialate geopolymers (Figs. 3a, 3b, and 4a). This could be the reason for ferrosialate specimens displaying higher compressive strength than sialate specimens, at all the stages of curing.

4 Conclusions

The following conclusions are drawn from the obtained results.

(i) For maximum strength gain in ferrosialate geopolymer mortars, advisable replacement of red mud is found to be 20% and 30% for oven curing and ambient curing regimes, respectively. And Synergy has to be found among the red mud content, curing type and curing temperature for optimum results.

(ii) Ferrosialate geopolymers gained higher early strength than sialate geopolymers. Also, ferrosialate geopolymer samples showed

53.34% higher maximum compressive strength than sialate geopolymer samples. This shows that the ferrosialate geopolymer performed better than sialate geopolymers.

(iii) Beyond 30% RM replacement leads to greatly increase the crystalline content and undissolved phases in the matrix, thereby hindering the geopolymerization process.

(iv) The oxide ratios of SiO_2/Al_2O_3 = 4.0 to 4.3, Na_2O/SiO_2 = 0.15 to 0.17 and Fe_2O_3/Al_2O_3 = 0.27 to 0.37 are found to be limits for favouring strength gain.

References

1 Davidivits J, *J Therm Anal*, 37 (1991) 1633.
2 Xu H & Van D J S J, *Int J Miner Process*, 59 (2000) 247.
3 Kumar S & Kumar R, *Synergising Red Mud and Grey Ash for Greener Geopolymers*, Paper presented at International Conferenceon Bauxite Residue Valorisation and Best Practices, Leuven, Belgium, 2004.
4 Davidovits J, Davidovits M & Davidovits F, *France*, FR Pat. 2012/056125, 2012.
5 Singh S, Aswath M U & Ranganath R V, *Constr Build Mater*, 177 (2018) 91.
6 Klauber C, Gräfe M & Power G, *Hydrometallurgy*, 108 (2011) 11.
7 Kumar A & Kumar S, *Constr Build Mater*, 38 (2013) 865.
8 Patel S & Pal B K, *Int J Latest Tech Eng Manag Appl Sci*, 4 (2015) 1.
9 Brunori C, Cremisini C, Massanisso P, Pinto V & Torricelli L, *J Hazard Mater*, 117 (2005) 55.
10 Hu Y, *Constr Build Mater*, 200 (2019) 398.
11 Kaze R C, Beleuk à Moungam L M, Cannio M, Rosa R, Kamseu E & Leonelli C, *J Clean Prod*, 199 (2018) 849.
12 Obonyo E A, Kamseu, Lemougna P N, Tchamba A B & Leonelli C, *Sustain*, 6 (2014) 5535.
13 Duxson P, Mallicoat S W, Lukey G C & Van D, *Colloids Surf A Physicochem Eng Asp*, 292 (2007) 8.
14 Cui Y, Wang D, Wang Y & Rui Y, *J Non Cryst Solids*, 511 (2019) 19.
15 Barbosa V F F, MacKenzie K J D & Thaumaturgo C, *Int J Inorg Mater*, 2 (2000) 309.
16 Lahoti M, Narang P, Tan K H & Yang E H, *Ceram Int*, 43 (2017) 11433.
17 Pouhet R, Cyr M & Bucher R, *Constr Build Mater*, 201 (2019) 421.
18 De Silva P, Sagoe-Crenstil K & Sirivivatnanon V, *Cem Concr Res*, 37 (2007) 512.
19 Xu H & Van D, *Ind Eng Chem Res*, 42 (2003) 1698.
20 IS 650: 1991- Standard sand for testing cement: specification.
21 Nath S K & Kumar S, *Constr Build Mater*, 233 (2020) 117294.
22 IS 4031: 1988 - Methods of physical tests for hydraulic cement.
23 Pilehvar S, Cao V D, Szczotok A M, Carmona M, Valentini L & Kjøniksen A L, *Constr Build Mater*, 173 (2018) 28.
24 X'Pert High Score Plus software, PANalytical BV, Almelo, Netherlands, 2012.
25 Choo H, Lim S, Lee W & Lee C, *Constr Build Mater*, 125 (2016) 21.
26 Sagoe-Crentsil K & Weng L, *J Mater Sci*, 42 (2007) 3007.
27 Lemougna P N, Tuo Wang, Tang Q & Min Cui X, *Constr Build Mater*, 131 (2017) 564.
28 He J, Zhang J, Yu Y& Zhang G, *Constr Build Mater*, 30 (2012) 80.
29 Hardjito D & Rangan B V, *Development and properties of low-calcium fly ash-based geopolymer concrete Research Report GC 1* (Curtin University of Technology) 2005.
30 North M R & Swaddle T W, *Inorg Chem*, 39 (2000) 2661.
31 Anseau M R, Leung J P, Sahai N & Swaddle T W, *Inorg Chem*, 44 (2005) 8023.
32 Weng T B L & Sagoe-Crentsil K, *Geopolymer 2002 Int Conf*, Melbourne, Australia, 2002.
33 Fletcher R A, MacKenzie K J D, Nicholson C L & Shimada, *J Eur Ceram Soc*, 25 (2005) 1471.
34 Ye N, Chen Y, Yang J, Liang S, Hu Y, Hu J, Zhu S, Fan W & Xiao B, *Cem Concr Res*, 101 (2017) 123.
35 Duxson P, Fernández-Jimenez A, Provis J L, Lukey G C, Palomo A & Van Deventer J S J, *J Mater Sci*, 42 (2007) 2917.
36 Provis J L & Van D J S J, *Chem Eng Sci*, 62 (2007) 2309.
37 Provis J L & Van D J S J, *Chem Eng Sci*, 62 (2007) 2318.
38 Scardi P, *Diffraction Analysis of the Microstructure of Materials*, (Springer-Verlag Berlin Heidelberg), 2004, ISBN 978-3-540-40519-1 .
39 Madsen I C, Scarlett N V Y & Kern A, *Zeitschrift Für Krist. - Cryst Mater*, 226 (2011) 944.
40 Lassinantti G M, Romagnoli M & Gualtieri A F, *J Eur Ceram Soc*, 35 (2015) 3167.
41 Mandal A K, Verma H R & Sinha O P, *J Clean Prod*, 162 (2017) 949.
42 Geng J J, Zhou M, Li Y, Chen Y, Han Y, Wan S, Zhou X & Hou H, *Constr Build Mater*, 153 (2017) 185.